Crossover from spherical particle Mie scattering to circular aperture diffraction

William R. Heinson, Amitabha Chakrabarti, and Christopher M. Sorensen*

Department of Physics, Kansas State University, 116 Cardwell Hall, Manhattan, Kansas 66506-2601, USA
**Corresponding author: sor@phys.ksu.edu*

Received June 17, 2014; revised September 3, 2014; accepted September 8, 2014;
posted September 8, 2014 (Doc. ID 214134); published October 7, 2014

This paper demonstrates the manner in which the Mie results for light scattering by a three-dimensional sphere of arbitrary size and refractive index crosses over to Fraunhofer diffraction by a two-dimensional circular aperture of the same radius in the limit of very large radius. Demonstration is feasible only because the graphical results are plotted in the manner of the Q-space analysis that plots scattered intensity versus the logarithm of the magnitude of the scattering wave vector rather than linear versus the scattering angle. © 2014 Optical Society of America

OCIS codes: (290.4020) Mie theory; (290.5825) Scattering theory; (050.1940) Diffraction.
http://dx.doi.org/10.1364/JOSAA.31.002362

1. INTRODUCTION

Light scattering by spheres is described by Mie theory [1–3], which allows for calculation of the differential and total scattering cross sections for all sizes and refractive indices. The only limitation to calculation lies in computational ability, but this ability has seen steady progress over the past four decades to the point where calculation for very large sizes and refractive indices can be accurately achieved. This opens the opportunity to look at the nature of scattering empirically in either detail, in various limits, or from different points of view.

The purpose of this brief paper is to study the crossover from spherical particle Mie scattering to Fraunhofer circular aperture diffraction in the limit of very large refractive spheres. More precisely, to quantify the extent of the crossover, the phase shift parameter

$$\rho = 2kR|m-1| \tag{1}$$

will be used. In Eq. (1) $k = 2\pi/\lambda$, where λ is the wavelength, R is the sphere radius, and m is the sphere refractive index relative to the medium. The limit of very large ρ will take us close to the geometric limit where the wavelength $\lambda \to 0$ and light propagates in straight lines, but not quite, since the wave nature of light is still in effect to cause diffraction. This geometric and diffraction optics regime is the physical optics limit [4] in which the electromagnetic nature of light is lost leaving its ray and wave natures.

The crossover from Mie theory to physical optics is illustrated well in the behavior of the total scattering cross section. When the phase shift parameter is less than $\rho \sim 3$, the total scattering is, generally speaking, well described by the Rayleigh formula with $k^4R^6|(m^2-1)/(m^2+2)|^2$ functionality [2,3]. When $\rho > 3$, the total scattering crosses over to an eventual geometric functionality of twice the projected area, $2\pi R^2$, with no refractive index or wavelength dependence. The factor of two is the so-called extinction paradox [2,3,5] related to the wave nature.

The crossover from Mie theory to physical optics is also illustrated well in the behavior of the differential scattering cross section in the Guinier regime [6]. The Guinier regime is when $qR \approx 1$, where

$$q = 2k\,\sin(\theta/2) \tag{2}$$

is the scattering wave vector magnitude at scattering angle θ. For small ρ the differential Mie scattering cross section follows the classic Guinier equation [7] for $qR < 1$:

$$dQ_{\mathrm{sca}}/d\Omega \sim 1 - \frac{(qR)^2}{5}. \tag{3}$$

When the phase shift parameter increases, this functionality remains valid but with the actual radius R replaced with an effective radius, R_e. The ratio of the effective radius to the true radius, R_e/R, increases initially with ρ then oscillates and damps to $R_e/R = 1.12$ in the limit $\rho \to \infty$ [6]. This large ρ limit is the physical optics limit. In this limit the large three-dimensional sphere acts like a two-dimensional circular obstacle, and Fraunhofer diffraction describes the forward scattering. The Fraunhofer diffraction intensity is given by [4]

$$I(q) = I(0)\left[\frac{2J_1(qR)}{qR}\right]^2, \tag{4}$$

where $J_1(x)$ is the first Bessel function. Expansion of Eq. (4) when $qR < 1$ yields

$$I(q) \approx I(0)(1-(qR)^2/4). \tag{5}$$

The Guinier analysis of Eq. (3) applied to the $\rho \to \infty$ limit of Eq. (5) would yield an effective radius for the Guinier analysis of $R_e/R = \sqrt{5/4} = 1.12$, which is the same as the large ρ Mie result. This shows that the Mie equations have a $\rho \to \infty$ limit consistent with physical optics in the Guinier regime.

Given the facts above illustrating that the Mie total scattering cross section and the differential cross section in the Guinier regime display the correct $\rho \to \infty$ limit, the purpose of this paper is to explore the behavior of the Mie differential cross section at all angles as the situation evolves from small to large ρ. To do this we will use an unconventional method to display the angular scattering dependency, the Q-space analysis [8]. Q-space analysis involves plotting the scattered intensity versus q, the magnitude of the scattering wave vector, on a log–log format, instead of the convention linear θ. The method was first applied to Mie scattering from spheres to uncover patterns in the scattering that involved power laws [9,10]. However, in that work the focus was on small to moderate phase shift parameters. Here we extend that work to much larger ρ values and uncover more power law patterns that have not been described before including reference [8]. These new power laws eventually lead to the first Bessel function due to circular aperture diffraction, Eq. (4).

2. RESULTS

Figure 1 shows Mie scattering intensity versus qR for a sphere of radius 103 μm, refractive index of $m = 1.05$, and light of wavelength 0.65 μm; hence, $\rho = 100$. Scattering was calculated using Philip Laven's freeware program MiePlot [11]. MiePlot is a simple yet robust interface built to use the famous Bohren and Huffman algorithm for Mie scattering [3,11]. This figure displays the characteristic Mie patterns in q-space [8–10]: a forward scattering lobe with no q functionality (hence no angular functionality) when $qR < 1$, a Guinier crossover near $qR \approx 1$, a rough power law of $(qR)^{-2}$ when $1 < qR < 1.2\rho$ (note the "sag" in the scattering curve below this power law), and a rough $(qR)^{-4}$ power law that approximately matches the envelope of the Rayleigh–Debye–Gans (RDG) formula for $(qR) > 1.2\rho$. The value 1.2ρ is an approximate empirical value. Not demonstrated in Fig. 1 is that this result is quasi-universal with ρ. That is, different combinations of the size parameter kR and refractive index lie fairly close together on this plot if the ρ is the same [10]. The RDG formula is the square of the Fourier transform of a sphere and as such

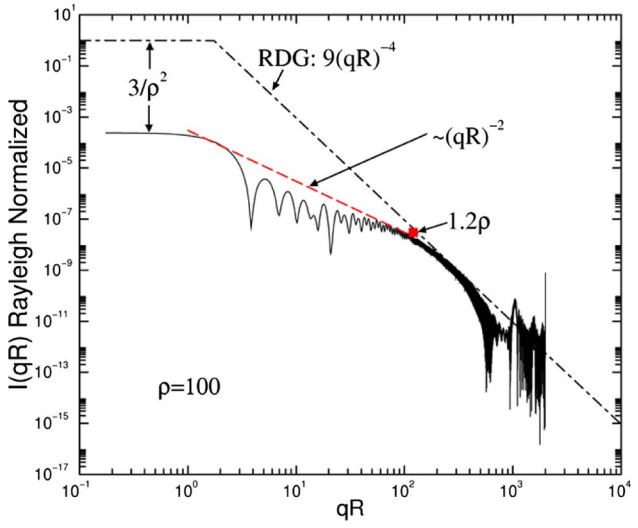

Fig. 1. Rayleigh normalized Mie scattering intensity versus qR for $\rho = 100$. Dot-dashed line is the envelope for the Rayleigh–Debye–Gans result for scattering from a $\rho = 0$ sphere.

describes Fraunhofer diffraction by a sphere. Furthermore, it is the $\rho = 0$ limit of Mie scattering. The Mie forward lobe intensity is smaller by a factor of ca. $3/\rho^2$ from the Rayleigh scattering value of the sphere.

Figure 2 shows scattering intensity versus qR for both $\rho = 0.4$ and 1200. To gain a wide range of qR values for a given ρ, the parameters kR and m for each ρ calculation varied greatly. Spheres of radii from 10 μm to 1.2 cm, wavelengths from 0.01 to 1.2 μm, and refractive indices ranging from $m = 1.0002$ to 1.6 were used, but all runs fell into two groups: those with phase shift parameter $\rho = 0.4$ and those with $\rho = 1200$. The $\rho = 0.4$ spheres fall in line with the envelope of the RDG formula for a sphere that includes Rayleigh scattering in the forward lobe and $I = 9(qR)^{-4}$ for large qR, as expected. The $\rho = 1200$ spheres have a q-independent forward scattering lobe decreased by a factor of ca. $3/\rho^2$ from the Rayleigh scattering value of the spheres, as observed in Fig. 1 for $\rho = 100$. For larger qR, however, the "sag" in the $(qR)^{-2}$ regime seen for $\rho = 100$ has developed into two new features. For $1 < qR < 30$ a $(qR)^{-3}$ regime appears. After that the functionality levels off to a flat plateau that rounds off near $qR \approx 1.2\rho$. Now the $(qR)^{-2}$ power law regime exists only as a line drawn tangent to the scattering at $qR \approx 1$ and 1.2ρ. At yet larger qR, the envelope functionality approximately regains the $9(qR)^{-4}$ behavior of the RDG, Fourier transform squared of the spherical shape.

Figure 3 shows detail of Fig. 2 confined to $qR < 100$. Plotted along with the spherical particle Mie scattering is the Fraunhofer diffraction for a two-dimensional circular aperture of the same diameter as the sphere, Eq. (4). There we see a strong coincidence of the Mie scattering and the circular aperture diffraction, especially for $qR < 30$. We conclude that in this qR range the $\rho = 1200$, three-dimensional spheres are acting like two-dimensional circular obstacles; Mie scattering is successfully crossing over to the physical optics limit.

The envelope of circular aperture diffraction, which can be obtained from Eq. (4) in the limit of large qR, is $(8/\pi)(qR)^{-3}$

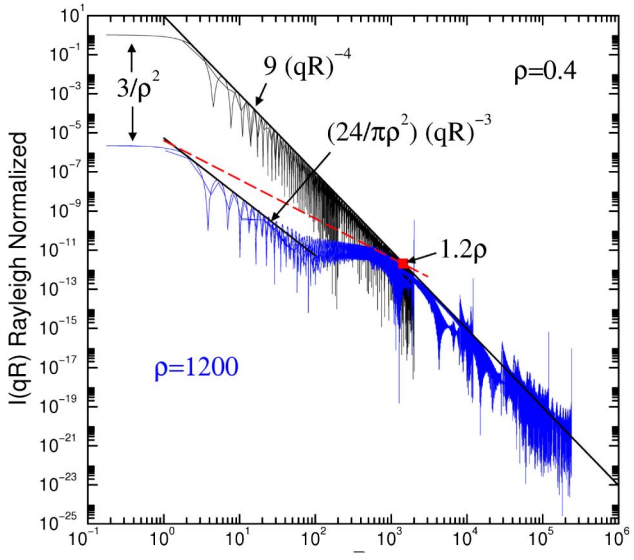

Fig. 2. Rayleigh normalized Mie scattered intensity versus qR for spheres with phase shift values of $\rho = 0.4$ and 1200. Solid black lines are envelopes for spherical particle RDG scattering $9(qR)^{-4}$, which is Fraunhofer diffraction for a three-dimensional sphere, and two-dimensional circular aperture Fraunhofer diffraction.

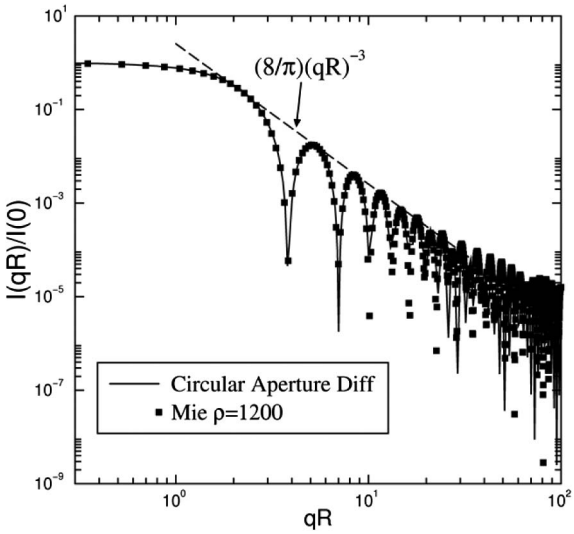

Fig. 3. Fraunhofer circular aperture diffraction from Eq. (4) (solid line), its envelope (dashed line), and spherical particle Mie scattering with phase shift value of $\rho = 1200$ (square points).

when the diffraction is normalized to unity at $qR \to 0$. This envelope is drawn as a dashed line in Fig. 3. Given that the forward scattering lobe is decreased by a factor of $3/\rho^2$ relative to Rayleigh scattering, the circular aperture diffraction envelope is $(24\pi/\rho^2)(qR)^{-3}$ when the forward scattering is normalized by Rayleigh scattering. This envelope is drawn as a solid line in Fig. 2.

3. CONCLUSION

In conclusion, Figs. 2 and 3 demonstrate that Mie scattering for three-dimensional spherical particles in the limit of very large phase shift parameter ρ crosses over to Fraunhofer diffraction by a two-dimensional circular aperture. Resaid: the Mie equations at $\rho = 0$ yield the Fourier transform of a sphere; at $\rho \to \infty$ they yield the Fourier transform of a circular aperture, and they effectively describe the crossover in between. This is certainly expected, but it is gratifying to see. Also, spheres at large ρ will deviate from two-dimensional diffraction, develop a flat plateau, and then near $qR \approx 1.2\rho$ regain the three-dimensional diffraction envelope of $(qR)^{-4}$.

Finally, it is important to remark that this crossover would be very difficult to detect and impossible to describe quantitatively without the Q-space analysis. The various power laws with qR that show graphically as straight lines on the log–log plots would all, when plotted versus the scattering angle θ, be difficult-to-distinguish curves.

ACKNOWLEDGMENTS

This work was supported by NSF grant AGM 1261651.

REFERENCES

1. G. Mie, "Beitrage zur Optik truber Medien speziel kolloidaler Metallosungen," Ann. Phys. **330**, 377–445 (1908).
2. H. C. van de Hulst, *Light Scattering by Small Particles* (Dover, 1981).
3. C. F. Bohren and D. R. Huffman, *Absorption and Scattering of Light by Small Particles* (Wiley, 1983).
4. E. Hecht, *Optics*, 2nd ed. (Addison-Wesley, 1987).
5. M. J. Berg, C. M. Sorensen, and A. Chakrabarti, "Extinction and the optical theorem. Part I. Multiple particles," J. Opt. Soc. Am. A **25**, 1504–1513 (2008).
6. C. M. Sorensen and D. Shi, "Guinier analysis for homogeneous dielectric spheres of arbitrary size," Opt. Commun. **178**, 31–36 (2000).
7. A. Guinier, G. Fournet, C. B. Walker, and K. L. Yudowitch, *Small Angle Scattering of X-Rays* (Wiley, 1955).
8. C. M. Sorensen, "Q-space analysis of scattering by particles: a review," J. Quant. Spectrosc. Radiat. Transfer **131**, 3–12 (2013).
9. C. M. Sorensen and D. J. Fischbach, "Patterns in Mie scattering," Opt. Commun. **173**, 145–153 (2000).
10. M. J. Berg, C. M. Sorensen, and A. Chakrabarti, "Patterns in Mie scattering: Evolution when normalized by the Rayleigh cross section," Appl. Opt. **44**, 7487–7493 (2005).
11. P. Laven, "Simulation of rainbows, coronas, and glories by use of Mie theory," Appl. Opt. **42**, 436–444 (2003).